IEEE Access
Multidisciplinary | Rapid Review | Open Access Journal

Received November 29, 2019, accepted December 10, 2019, date of publication December 16, 2019,
date of current version December 26, 2019.

Digital Object Identifier 10.1109/ACCESS.2019.2959880

Fabric Defect Detection Method Combing Image Pyramid and Direction Template

HUOSHENG XIE, YAFENG ZHANG, AND ZESEN WU
School of Mathematics and Computer Science, Fuzhou University, Fuzhou 350591, China

Corresponding author: Huosheng Xie (xiehs@fzu.edu.cn)

This work was supported by the National Natural Science Foundation of China under Grant 61473330 and Grant 61801121.

ABSTRACT Focusing on the fabric defect detection with periodic-pattern and pure-color texture, an algorithm based on Direction Template and Image Pyramid is proposed. The detection process is divided into two stages: model training and defect localization. During the model training stage, we construct an Image Pyramid for each fabric image that does not contain any defects. Then, Stacked De-noising Convolutional Auto-Encoder (SDCAE) is used for image reconstruction, its training sets are created by randomly extracting image blocks from image pyramid, which makes the feature information of the image block more abundant and the reconstruction effect of the model more remarkable. During the defect localization stage, the image to be detected is divided into a number of blocks, and is reconstructed by using the trained SDCAE model. Then, the candidate defective image blocks are roughly located by using the Structural Similarity Index Measurement after the image reconstruction. Subsequently, direction template is introduced to solve the problem of fabric deformation caused by factors such as fabric production environment and photographic angle. We select the direction template of the images to be detected, filter the candidate defective blocks, and further reduce false detection rate of the proposed algorithm. Furthermore, there is no need to calculate size of periodic-pattern during detection for periodic textured fabric. The algorithm is also suitable for defect detection for pure-color fabrics. The experimental results show that the proposed algorithm can achieve better defect localization accuracy, and receive better results in detection of pure-color fabrics, compared with traditional methods.

INDEX TERMS Fabric defect detection, direction template, image pyramid, stack de-noising convolutional auto-encoder, similarity measure.

I. INTRODUCTION

Fabric defect detection is an important part of product quality management. In many textile industries, defect detection is still relying on labor inspection. Inspectors can easily find defects in fabrics by direct observation, but prolonged observation can easily fatigue human eyes and lead to an increasing number of inadvertently missed defects. Therefore, it is of great significance to study the application of computer vision technology [1] in automatic detection. However, due to the wide variety of defects (more than 70 categories of fabric defects [2]), distinct composition of various wallpaper groups of fabric texture, and similarity in shape between defects and background texture, it is difficult to develop an algorithm suitable for all kind of texture patterns and defect.

The associate editor coordinating the review of this manuscript and approving it for publication was Fan Zhang.

Currently, fabric defect detection methods are mainly based on the analysis of digital image features of fabrics. Image blocking method is widely used in existing fabric defect detection. These methods directly segment the images to be detected, which causes the feature information contained in the image to be easily damaged. Although setting the image block size to be the same as the periodic-pattern can alleviate the problem to some extent, its period calculation is complicated, and the positioning accuracy still needs to be improved. Because pure-color fabrics have no periodic texture, the existing defect detection methods for periodic texture fabrics are ineffective in the detection of pure-color fabrics. It is challenging to develop algorithms that can be used to detect defects in periodic-pattern fabrics and pure-color fabrics with wide variety of textures and defect types.

In view of this, a fabric defect detection method based on image pyramid and direction template is proposed in

this paper. By introducing image pyramid, the algorithm can be applied to defect detection of periodic texture fabric, and there is no need to calculate the size of periodic-pattern. The direction template is introduced to further reduce false detection rate. The algorithm first constructs an Image Pyramid for fabric images that do not contain any defects. The process will result in a set of images with gradually reduced resolutions of the fabric image. Then, we randomly slide the window in each layer of the image in the image pyramid to get image blocks, and use these image blocks as the input to the image reconstruction model. Subsequently, we train the model, get the output images, divide input and output images into blocks, calculate a similarity measure matrix of them, and locate defective image blocks roughly. Finally, we construct the direction template set of the input images, calculate the difference between the ''rough-positioning'' blocks and its corresponding direction template, and locate the defective blocks finely.

The contributions of this paper are as follows:

1. In this study, a novel fabric defect detection algorithm using Image Pyramid and Direction Template is proposed. The algorithm can effectively detect and locate defects in periodic-texture fabrics with relatively small train dataset. The experimental results has shown a promising result of 69.58% F-measure index for the standard Periodic-pattern Fabric database,[1] outperforming existing methods.
2. In this study, self-similarity and local-similarity of non-defective areas of periodic texture and pure-color texture are used to distinguish between defect areas and non-defect areas. The introduction of Image Pyramid makes image blocks with fixed block size contain more feature information, there is no need to calculate the size of periodic-pattern and the Direction Template matching method is used to improve the detection accuracy.
3. In this study, the proposed method is also used in the defect detection of pure-color fabrics, and we have achieved F-measure index of 80.65% with the TILDA dataset.[2]

The remaining parts of this paper are organized as follows. Related works and state-of-the-art algorithms are presented in Section II; the proposed algorithm based on the Image Pyramid and Direction Template is presented in Section III; experimental results and analysis are given in Section IV; final remarks and future works are given in Section V.

II. RELATED WORK

Fabrics can be categorized into two types of fabrics based on texture patterns: 1) fabrics having basic structures with simple patterns, i.e., pure-color fabrics. 2) fabrics with complex periodic patterns, i.e., periodic-pattern fabrics;

Common approaches used for detecting defects in pure-color fabrics are: 1) statistical analysis methods, including gray-level co-occurrence matrix [3], histogram [4] and mathematical morphology [5]; 2) spectrum analysis methods, including Fourier transformation [6], wavelet transformation [7] and Gabor filtering [8]; 3) learning methods, for example, neural networks [9]; 4) structural methods, for example, structural approach [10]; 5) model methods, including autoregressive model [11], Markov random field [12] and so on. Among them, statistical analysis and spectrum analysis methods are vulnerable to noise, poor anti-interference, and poor results from fabric image with large defect areas. Ngan [13] proposed to perform image preprocessing using wavelet transformation, so that defective areas can be located by comparing the differences between template images and images to be detected. However, it can be problematic for the algorithm, if images are slightly tiled, even after using image correction and/or cyclic shift. It is also challenging for the algorithm to deal with skewed images. Structural methods require high quality sample images, and the applicability of the method is limited. When using machine learning methods, features are self-learned and classified by deep-learning neural networks, or features can be extracted from the use of the combination of traditional feature engineering techniques and machine learning methods. However, deep learning method generally requires a large amount of training data, and there are only few publically available datasets, currently. In order to obtain sufficient training data, [14], [15] use their own fabric datasets(a fabric defect dataset created by an on-loom fabric imaging system [14] and a fabric defect dataset collected by the authors [15]) to train neural networks. On the other hand, [16], [17] use the image blocking method to expand the size of training data and then to train neural networks to identify defect contained in these image blocks, thus locating the defective area. [18] gets the local image blocks of the original images (the size is 1280×1024) manually that only contain one fabric defect type. The size of the local images is 227×227. And then uses a compressed sensing technology to expand these local images as the training data for Convolutional Neural Network (CNN). Meanwhile, [19], [20] introduced the unsupervised learning model DAE to solve the data labeling problem and defect localization (in contrast, supervised learning requires pre-labeled data), and the method only needs a few non-defective images to train models. However, the performance of the unsupervised learning algorithm is affected by the reconstruction result of the DAE model. The detection results often contain some false detection area.

Conventional defect defection methods for periodic-pattern fabrics are often based on the calculation of image features using Golden Image Subtraction (GIS) [21], Wavelet Preprocessed Golden Image Subtraction (WGIS) [22] or Gabor golden Image Subtraction method (GGIS) [23] and Image Decomposition method(ID) techniques [24]. Since fabrics are often prone to stretching problems, it is infeasible to find a template suitable for all images. GGIS is a template image subtraction method that uses a Gabor filter to preprocess template images in order to extract features. It relies on the use of genetic algorithms to determine appropriate

[1] https://ytngan.wordpress.com/codes/

[2] https://lmb.informatik.uni-freiburg.de/resources/datasets/tilda.en.html

parameters for Gabor filter, which is often cumbersome to calculate. Image Decomposition requires to separate an image into a uniform background and a defective foreground, so as to filtering defects. However, the process of formulating the optimization problem is rather complex, and several empirical parameters, based on field experiments, are often needed for building the model. Reference [25] enhances contrast between defective area and non-defective area in each fabric image by generating a saliency map during the preprocessing stage, then extracts features from the preprocessed images, and finally sends the extracted features to a SVM classifier for detection. Fabrics having periodic-pattern are more common on the market. However, the accuracy of the traditional algorithms is far lower than the satisfaction level required by textile industries.

In recent years, researchers have proposed several improved algorithms for periodic-pattern fabric defect detection, driven by the market demands, for example, fabric defect detection based on similarity relationship – Elo Rating (ER) [26], fabric defect detection method based on similarity relationship [27], fabric defect detection method based on local optimal analysis [28], and fabric defect detection method based on template correction and low rank decomposition [29]. These methods, including ER, [27], [28], and [29] achieve defect detection at block level. The ER algorithm uses an Elo rating method for defect detection in the spirit of sportsmanship, i.e., fair matches between partitions in an image. The algorithm assigns an initial Elo point to each partition. Matches are performed between partitions and Elo points are adjusted accordingly. The losing partitions with lower Elo point are consider as defective partitions. Defect regions are identified after all matches. The algorithm is a supervised learning algorithm and it is computationally intensive. In [27], an image block clustering technique is used to identify defect regions. The algorithm first divides an image into blocks. The size of each block is determined by ''one agreement two'' method. Second, the algorithm generates a similarity matrix for the image by calculating correlation coefficients of each image block. Thereafter, image blocks are clustered into defective and non-defective classes by calculating a transfer closure matrix of the similarity matrix. In [29], the authors proposed a defect detection algorithm that makes corrections of an image to be detected based on non-defective image template. The defect detection is done by segmenting salient maps generated by a sparse matrix of a low-rank correction decomposition model.

At present, most of the defect detection algorithms have a limited applicability. The methods for fabric defect detection designed for the pure-color fabrics are not suitable for periodic-pattern fabrics, and vice versa. The situation can be improved by introducing auto-encoder to image reconstruction. However, in traditional methods, training data directly comes from non-defective images, which results in the image block with fixed block size containing less features and the accuracy of the algorithm is reduced. To this end, a fabric defect detection method combining Image Pyramid [30] and Direction Template is proposed. The effectiveness and performance of the proposed algorithm have been evaluated using widely adopted fabric dataset. The algorithm achieved up to 69.58% on F-measure index, which outperforms existing methods.

III. THE PROPOSED METHOD BASED ON IMAGE PARAMID AND DIRECTION TEMPLATE

Traditional fabric defect detection methods are mainly based on the analysis of digital image features of fabrics. Due to the wide variety of texture and defect types exist in fabrics, it is challenging to develop an algorithm that can locate defect areas accurately. In this paper, we use an improved SDCAE model as an image reconstruction model to reconstruct the images to be detected and we determine the defect area in the image by means of the similarity measurement.

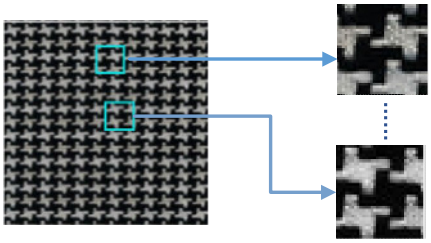

FIGURE 1. Extraction of 32*32 image blocks from original image (256*256) (make the image bigger for easy observation).

Additionally, traditional defect detection methods use image blocks extracted from non-defective images. These methods randomly extract fixed-size image blocks from a non-defective image (as shown in Figure 1), that are used for training models. In order to embody more image feature information, the size of image blocks must be sufficiently large, but the accuracy of defect location will be affected. How to include more image feature information in an image block of a fixed-size, while ensuring accuracy of defect localization is another primary focus of this study. In response to this challenge, two novel ideas are developed: Image Pyramid and Direction Template. Before training the image reconstruction model, the image pyramid is used to increase the feature information contained in the image block. When locating the defect area, the direction template matching method is used to further filter the defect blocks (we call it ''fine-positioning'') to improve the accuracy of the proposed method. To this end, an improved SDCAE-based image reconstruction method incorporated with Image Pyramid and Direction Template is proposed for effective and efficient defect detection in periodic-pattern fabrics and pure-color fabrics.

A. IMAGE PYRAMID

Image Pyramid is a way of representing an image on multi-level. The bottom of the pyramid is the image of its original size. The layers from the bottom to the top of the pyramid are obtained by recursively down sampling each adjacent

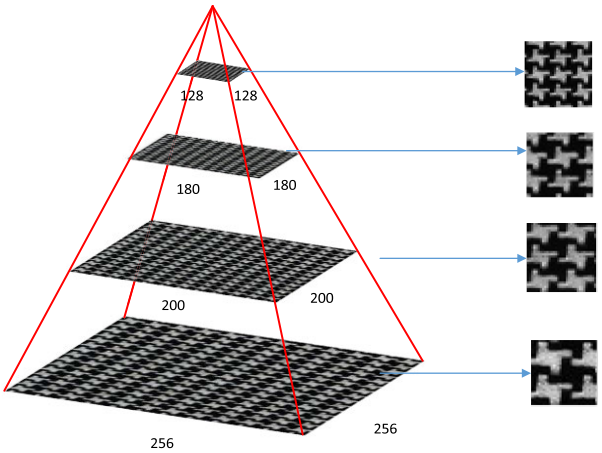

FIGURE 2. 32*32 image blocks extracted from each layer of the image pyramid.

layer (as shown in Figure 2). As it can be seen from the figure, with the increasing number of layers, image resolutions decrease gradually, and the detailed feature information decreases gradually, but the global feature information increases (block size is consistent across all layers). It is worth noting that the number of layers must be carefully selected. When the number of layers is too few, the feature information contained in each image block tends to be overlapping, when the number of layers is too many, it is easy to exclude feature information. In the experiments, a four-layer image pyramid is used. In each layer of the image pyramid, image blocks are randomly extracted with a r ∗c size sliding window. The number of image blocks is proportional to the size of each layer in the image pyramid. A total of N image blocks is extracted for training the image reconstruction model (see Figure 7 for details). The set of image blocks extracted from all layers of the image pyramid (with the same size) contain much greater, multi-level, feature information, that can be used to construct a more robust model.

B. IMAGE RECONSTRUCTION MODEL

Auto-Encoder (AE) is an unsupervised learning algorithm, which uses the structure of neural network to encode and decode information. It is a widely adopted algorithm in the field of image restoration, data compression and image generation. In this paper, Stacked De-noising Convolutional Auto-Encoder (SDCAE) [31] is used as image reconstruction model. It is a variant of conventional AE. It uses stack-connected convolution layers to replace hidden layers of a conventional AE, so that the model retains the advantages of Convolutional Neural Network (CNN) structure: local perception and value sharing, which can greatly reduce the number of model parameters, thus, making the model more time-efficient for training and testing. SDCAE also retains the ability of aggregating spatial information and feature dimension information of AE, which is useful for improving image reconstruction quality of the model. The image reconstruction model consists of two parts: encoder and decoder. Model parameters and network depth for each convolution layer are carefully adjusted before training.

As shown in Figure 3, the steps for training the network are as follows. Extracted image blocks (denoted as X) are used as the input for the model. A random noise is added to each image block x (with r ∗ c size) in X. After the first three rounds of convolution-pooling operations (encoder) and the last three rounds of up sampling-convolution operations (decoder), the output y of the network is obtained, $y = F(x)$. When X of N * image blocks is processed in the same way, we can obtain the set of all the reconstructed image blocks (denoted as Y). The loss function is defined as the Euclidean distance between the input image block set X and the reconstructed image block set Y. By minimizing the value of the loss function, the local minimal point can be found, which indicates the convergence of the model and completes the weight training for each layer.

C. SIMILARITY MEASURE AND "ROUGH-POSITIONING"

After training the image reconstruction model, we can use the model to reconstruct the image to be detected. First, we need to divide the fabric image to be detected (denoted as I) into several r*c-sized image blocks. These image blocks are used as inputs to the image reconstruction model to obtain the reconstructed image (denoted as I′), $I' = F(I)$. Figure 4 (a) and (b) show the partial results before and after the reconstruction of defective image blocks, and Figure 4 (c) and (d) show the results for non-defective image blocks. As it can be seen from Figure 4, the reconstruction of non-defective image blocks is highly similar before and after reconstruction. (We call it "self-similarity") In contrast, there are significant differences between the defective image blocks and reconstructed defective image blocks. Based on this observation, defects can be identified by comparing image blocks before and after reconstruction. In this paper, Structural Similarity Index Measurement (SSIM) [32] is used to quantify the differences between defective blocks and non-defective blocks. The formulas for calculating the SSIM for two image blocks P and Q are as follows:

$$\mathrm{SSIM}(P, Q) = \frac{(2u_P u_Q + c_1)(2\delta_{PQ} + c_2)}{\left(u_P^2 u_Q^2 + c_1\right)\left(\delta_P^2 + \delta_Q^2 + c_2\right)} \quad (1)$$

where u_P and δ_P^2 are the average and the variance of P, respectively; u_Q and δ_Q^2 are the average and the variance of Q; δ_{PQ} is the covariance of P and Q; c_1 and c_2 are constants. The value of SSIM ranges in [0, 1]. If the value of SSIM equals 1, the two image blocks are highly similar.

The detailed steps for calculating the similarity are as follows:

First, we have to consider the block of the image to be detected I and the reconstructed image I′(the output image

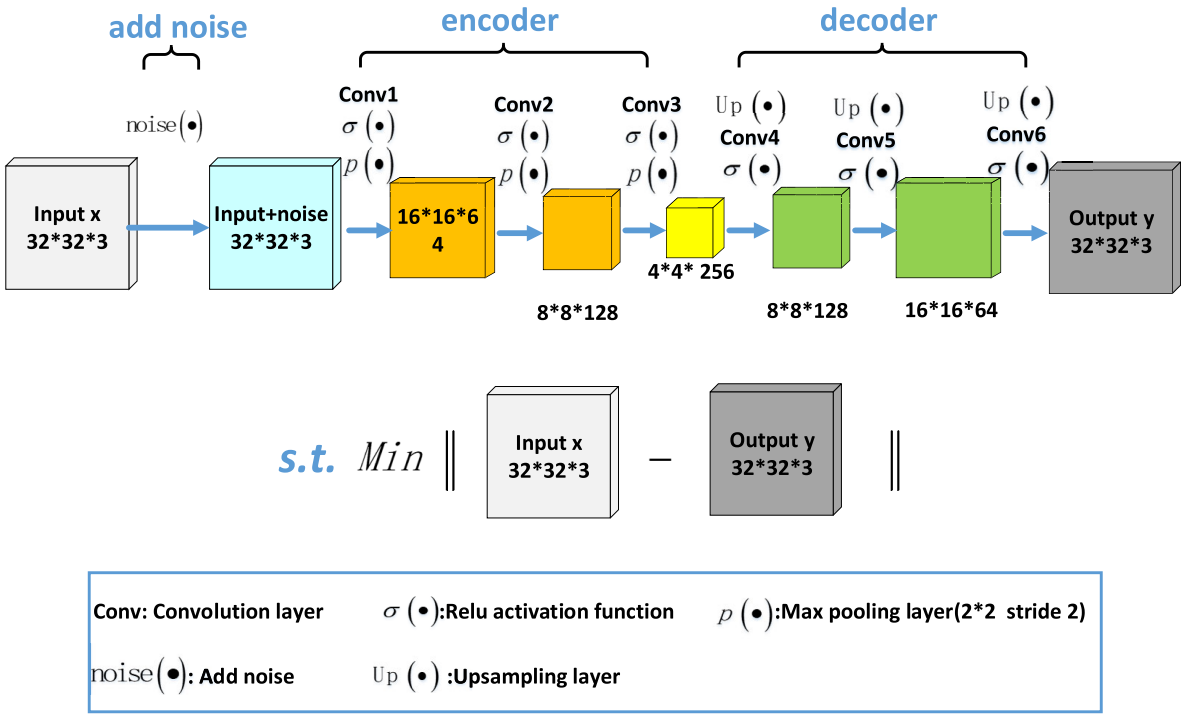

FIGURE 3. SDCAE Image reconstruction model.

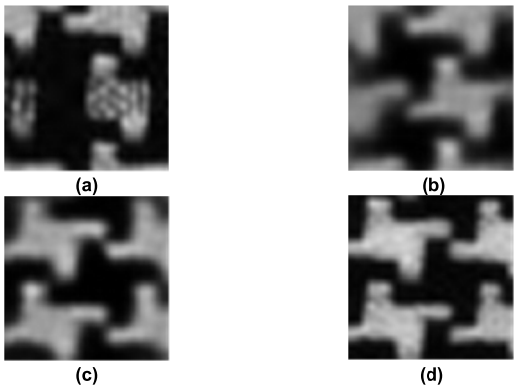

FIGURE 4. (a)Defective image block. (b)The image block of (a) after reconstruction. (c) Non-defective image block. (d) The image block of (c) after reconstruction.

of image reconstruction model), defined as:

$$\mathrm{I} = \begin{pmatrix} B_{1,1} & \cdots & B_{1,n'} \\ \vdots & \ddots & \vdots \\ B_{m',1} & \cdots & B_{m',n'} \end{pmatrix} \quad \text{and } \mathrm{I}' = \begin{pmatrix} B'_{1,1} & \cdots & B'_{1,n'} \\ \vdots & \ddots & \vdots \\ B'_{m',1} & \cdots & B'_{m',n'} \end{pmatrix}$$

The image I and I′ are divided into $\mathrm{m}' * \mathrm{n}'(m' = \lfloor \frac{\mathrm{R}}{r'} \rfloor, n' = \lfloor \frac{\mathrm{C}}{c'} \rfloor)$ sub-image blocks, where the sub-image block size is $\mathrm{r}' * c'$.

If the size of image blocks is too big, the defect area location in image block will be inaccurate, and if r' , c' are too small, it is hard to detect those blocks, which contain large defective area, and the localization accuracy of defects area will be poor. Thus, a 16 * 16 size image block is considered to be an appropriate size, that can cover most of defect areas with better localization accuracy.

Subsequently, the similarity measure matrix for I and I′, are calculated, denoted as $\mathrm{S} = \begin{pmatrix} s_{1,1} & \cdots & s_{1,n'} \\ \vdots & \ddots & \vdots \\ s_{m',1} & \cdots & s_{m',n'} \end{pmatrix}$, where $s_{i,j} = \mathrm{SSIM}\left(B_{i,j}, B'_{i,j}\right) \left(1 \le i \le m', 1 \le j \le n'\right)$.

Finally, a S-matrix block histogram of fabric image and a threshold T_s are collectively used to separate defective blocks and non-defective blocks; If $s_{i,j} \le T_s$, the image block $B_{i,j}$ is considered as an image block that potentially contains defect, i.e., ''rough-positioning.''

D. ''FINE-POSITIONING'' BASED ON DIRECTION TEMPLATE

After the similarity measurement, the accuracy of the algorithm can be further improved. Because the texture of adjacent non-defective image blocks in selected direction is similar (we call it ''the local-similarity'') and the texture difference between the defective image block and the direction template is large, the direction template matching method is used to further distinguish whether the ''rough-positioning'' defective block is a real defective block.

1) THE SELECTION OF TEMPLATE

Template can be horizontal, column, diagonal or global. For an image that is organized in block matrix, the average of image blocks in horizontal, vertical, diagonal and global

$A_{1,1}$	$A_{1,2}$	$A_{1,3}$	$A_{1,4}$
$A_{2,1}$	$A_{2,2}$	$A_{2,3}$	$A_{2,4}$
$A_{3,1}$	$A_{3,2}$	$A_{3,3}$	$A_{3,4}$
$A_{4,1}$	$A_{4,2}$	$A_{4,3}$	$A_{4,4}$

FIGURE 5. Schematic diagram of block images.

directions are calculated respectively and selected as templates. In this paper, the selection of the direction template was based on the analysis results from empirical studies. Taking a 4∗4 block image as an example (as shown in Figure 5), the template for each direction is calculated as follows:

Horizontal template set HT $= \{\bar{H}_j\}_{j=1}^{4}, \bar{H}_j = \frac{1}{4}\sum_{i=1}^{4} A_{i,j}$;

Column template set CT $= \{\bar{C}_i\}_{i=1}^{4}, \bar{C}_i = \frac{1}{4}\sum_{j=1}^{4} A_{i,j}$;

Diagonal template set AT $= \{\bar{T}_m\}_{m=1}^{7}, \bar{T}_m = \frac{1}{7}\sum_{i-j=m-4,1\le i,j\le 4} A_{i,j}$;

Anti-diagonal template set OT $= \{\bar{O}_m\}_{m=1}^{7}, \bar{O}_m = \frac{1}{7}\sum_{i+j=m+1,1\le i,j\le 4} A_{i,j}$;

Global template GT $= \frac{1}{16}\sum_{1\le i,j\le 4} A_{i,j}$.

Due to problems in the textile production environment and shooting angles, the values of column templates, horizontal templates, diagonal templates, anti-diagonal templates, and global templates may shift and stretch, which may result in the similarity values between defect-free image blocks and these direction templates are very different. For different data sets, the situations of shift and stretch may be different, and we need to calculate the degree of distortion of the images in each direction for each dataset and to select the most appropriate direction template.

(1) We randomly select N′* non-defective images from the dataset and calculate the template $\bar{H}_j, \bar{C}_i, \bar{T}_m, \bar{O}_m, \overline{GT}$, of each image in all directions.

(2) Calculate the average of the similarity value between the image blocks and the templates in each direction:

$$S_H = \frac{1}{m' \times n'} \sum_{j=1}^{n'} \sum_{i=1}^{m'} ssim(A_{i,j}, \bar{H}_j)$$

$$S_C = \frac{1}{m' \times n'} \sum_{i=1}^{m'} \sum_{j=1}^{n'} ssim(A_{i,j}, \bar{C}_i)$$

$$S_A = \frac{1}{m' \times n'} \sum_{m=1}^{m'+n'-1} \sum_{i-j=m-n'} ssim(A_{i,j}, \bar{T}_m)$$

$$S_O = \frac{1}{m' \times n'} \sum_{m=1}^{m'+n'-1} \sum_{i+j=m+1} ssim(A_{i,j}, \bar{O}_m)$$

$$S_G = \frac{1}{m' \times n'} \sum_{i=1}^{m'} \sum_{j=1}^{n'} ssim(A_{i,j}, \overline{GT})$$

(3) Select the direction template with the largest mean of similarity value of N' image:

$$T = \arg \underset{direction}{MAX} \left\{ \frac{1}{N'}\sum_N, S_H, \frac{1}{N'}\sum_N, S_C, \frac{1}{N'}\sum_N, S_A, \frac{1}{N'}\sum_N, S_O, \frac{1}{N'}\sum_N, S_G \right\}$$

where $\frac{1}{N'}\sum_N, S_H$ is the mean of the similarity values in horizontal direction of the N′* images, Column direction, diagonal direction, anti-diagonal direction and so on.

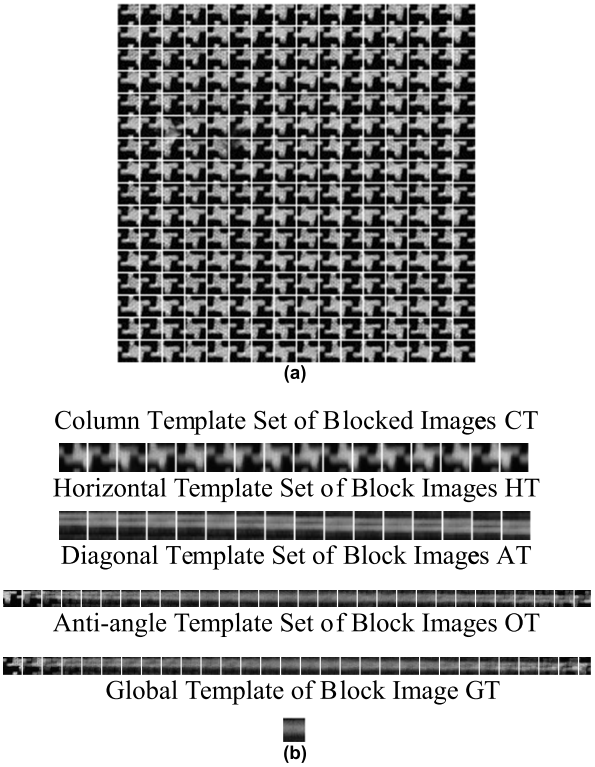

FIGURE 6. (a)Image block to be detected. (b) Template of the image (a) to be detected in all directions.

Figure 6(a) is a 16*16 block image, Figure 6(b) shows the templates in all direction, the similarity between the image block and its corresponding column direction template is the largest, which is the same as the result of the selection of template, the largest mean of similarity value on star type fabrics is the column direction template, because the images displayed in our dataset have little shift and stretching in the column direction. Therefore, the column direction template is selected as the reference template for ''fine positioning'' on star type fabrics.

2) ''FINE-POSITIONING'' METHOD

For each ''rough-positioning'' image block, the algorithm calculates the difference between ''rough-positioning'' image block $C_{i,j}$ and its corresponding direction template $\bar{C}_j$. If $\bar{C}_j$ is a defective image block, dist $\left(C_{i,j}, \bar{C}_j\right)$ will be larger than the threshold T_d. Conversely, dist $\left(C_{i,j}, \bar{C}_j\right)$ will be smaller

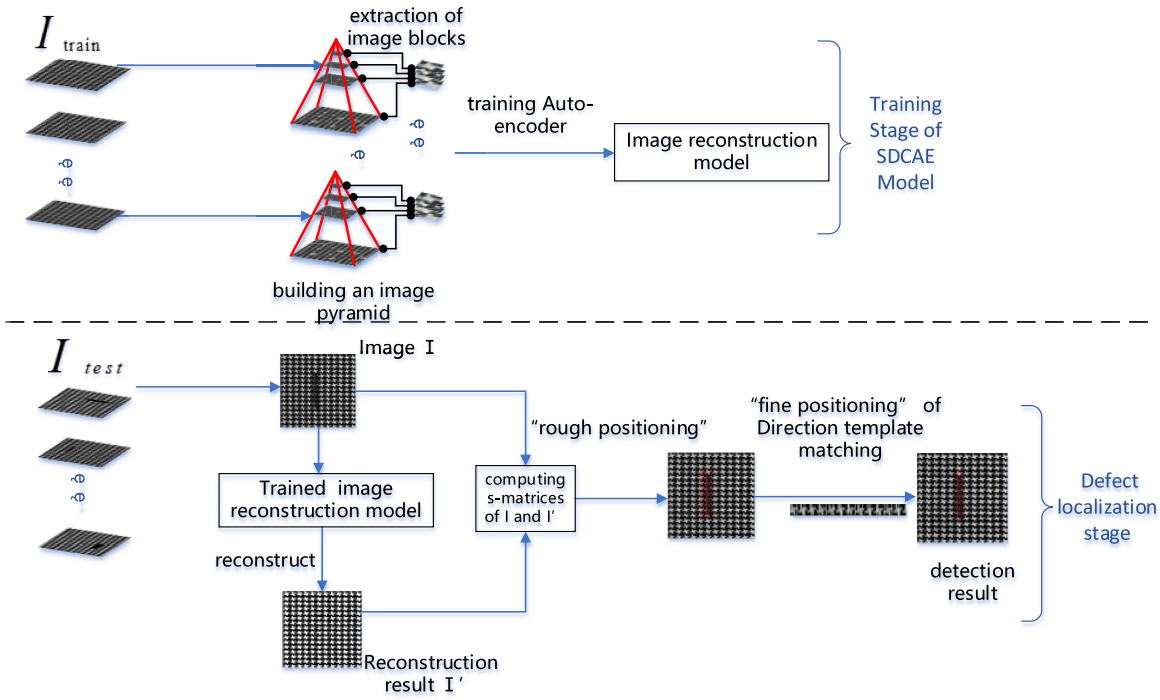

FIGURE 7. Flow chart of fabric defect detection method.

than T_d, if $C_{i,j}$ is a non-defective block. This filtering can significantly lower the false detection rate. The steps of the direction template "fine-positioning" method are as follows: (1) Generate a block matrix for each image to be detected; (2) Construct direction templates of horizontal, column, diagonal, anti-diagonal and global for each blocked-image and then select the best direction template T with the highest similarity values; (3) Calculate the differences between the results obtained from the "rough-positioning" process and the selected direction templates. The comparison results in an improved defect block localization, hence "fine-position."

E. THE PROCEDURE OF THE PROPOSED FABRIC DEFECT DETECTION METHOD BASED ON IMAGE PYRAMID AND DIRECTION TEMPLATE

As shown in Figure 7, the process is twofold: (1) training image reconstruction model and (2) defect localization.

The training stage of image reconstruction model:

Input: L_{train}* non-defective images (including 24 * star images, 28 * box images, 29 * dot images, with 256*256 image size).

Output: Trained Image Reconstruction Model F (∗).

Step1: For non-defective images (denoted as I_{train}), an image pyramid (denoted as g ∈ G) is built for each image, by recursively down sampling its immediate layer below, three times, i.e., a four-layer image pyramid;

Step2: Extract N* image blocks with r ∗ c size from G to form image block set X (for each layer image of G, the sliding window with r ∗ c size is used to walk randomly, and the image blocks are segmented. On average, one pyramid layer of an image is segmented into $\lfloor N/L_{train}/4 \rfloor$* image blocks);

Step3: Use the improved SDCAE as an image reconstruction model, and use the image block set X as the inputs for the SDACE. The training process terminates when the network of SDACE reaches its convergence point. The trained image reconstruction model is denoted as F (∗).

Defect location stage:

Input: L_{test}* images to be detected with R ∗ C size (including 25 * star images, 26 * box images and 30 * dot images, with 256*256 image size); and the trained image reconstruction model, F (∗).

Output: Detection result of L_{test} images.

Step1: Each image (denoted as A) in L_{test} is divided into uniform blocks of size r ∗ c, i.e., $A = \begin{pmatrix} A_{1,1} & \cdots & A_{1,n'} \\ \vdots & \ddots & \vdots \\ A_{m,1} & \cdots & A_{m,n} \end{pmatrix}$, where $m = \lfloor \frac{R}{r} \rfloor$, $n = \left\lfloor \frac{C}{c} \right\rfloor$;

Step2: Each image block $A_{i,j} \in A$, $(1 \le i \le m, 1 \le j \le n)$ is fed into SDCAE model, and the corresponding reconstructed image block $A'_{i,j}$ is obtained, $A'_{i,j} = F(A_{i,j})$, where $A' = \begin{pmatrix} A'_{1,1} & \cdots & A'_{1,n} \\ \vdots & \ddots & \vdots \\ A'_{m,1} & \cdots & A'_{m,n} \end{pmatrix}$;

Step3: Re-block A and A′ according to r′*c′ ($r' \ll r, c' \ll c$) size, respectively, as $A = \begin{pmatrix} B_{1,1} & \cdots & B_{1,n'} \\ \vdots & \ddots & \vdots \\ B_{m',1} & \cdots & B_{m',n'} \end{pmatrix}$, $A' = \begin{pmatrix} B'_{1,1} & \cdots & B'_{1,n'} \\ \vdots & \ddots & \vdots \\ B'_{m',1} & \cdots & B'_{m',n'} \end{pmatrix}$, where $m' = \lfloor \frac{R}{r'} \rfloor$, $n = \lfloor \frac{C}{c'} \rfloor$;

Step4: Calculate the similarity measure matrix of A and A′, marked as $S = \begin{pmatrix} s_{1,1} & \cdots & s_{1,n'} \\ \vdots & \ddots & \vdots \\ s_{m',1} & \cdots & s_{m',n'} \end{pmatrix}$, where $s_{i,j} = \mathrm{SSIM}\left(B_{i,j}, B'_{i,j}\right) \left(1 \le i \le m', 1 \le j \le n'\right)$;

Step5: Construct a structural similarity histogram of S, determine the threshold T_s. If $s_{i,j}$ is smaller than the threshold T_s in S, the image block $B_{i,j}$ is initially considered as a defect block $C_{i,j}$.

Step6: Construct and select the direction template T, e.g. column template, which is marked as $T = \bar{C}_j = \frac{1}{m'} \sum_{i=1}^{m'} B_{i,j}$;

Step7: Determine the distance threshold T_d, and calculate the difference value $\mathrm{dist}\left(C_{i,j}, \bar{C}_j\right) = \left\| C_{i,j} - \bar{C}_j \right\|$, if $\mathrm{dist}\left(C_{i,j}, \bar{C}_j\right)$ is greater than T_d, then $C_{i,j}$ is considered as an image block containing defects;

Step8: Traverse the set of L_{test} images, each image is processed in Step 2∼7, and the detection results of the corresponding L_{test} images are thereafter obtained.

IV. RESULTS AND ANALYSIS

A. DATASET AND EXPERIMENTAL ENVIRONMENT

The Periodic-pattern Fabric database and the TILDA dataset are selected to evaluate our method. The experimental environment consists of a LZ-748GT workstation configured with Intel E5-2600 CPU (2200 MHz), 32GB RAM and a Nvidia 16GB TITAN XP GPU. The software environment consists of python 3.6, Tensorflow-GPU.version 1.1, and CUDA 9.0.

1) THE PERIODIC-PATTERN FABRIC DATABASE

The Periodic-pattern Fabric database, provided by Prof. Ngan, University of Hong Kong [13], contains three types of textured fabrics: dot, star and box. Each type of fabric contains 5 to 6 defect types. The database contains fabrics with a visible periodic structure and is used to evaluate the performance of the proposed algorithm for periodic patterned fabrics.

2) THE TILDA DATASET

TILDA is a Textile Texture Database which was developed within the framework of the working group Texture Analysis of the DFG's (Deutsche Forschungsgemeinschaft) major research programme "Automatic Visual Inspection of Technical Objects." The database contains a total of eight representative textiles, three of which are pure-color textured fabric images: Silk with very fine structure (we call it "data1"), Unprinted rayon (we call it "data2"), Low variation of random structural materials (Such as wool or jute, we call it "data3"). The resolution of the image is 512*768. The TILDA dataset is used to evaluate the effectiveness of the proposed algorithm for pure-color fabrics, the TILDA dataset is used.

B. TRAINING IMAGE RECONSTRUCTION MODEL

In the experiments, the hyperparameters of image reconstruction model are configured as shown in Table 1.

TABLE 1. Super parameter setting.

Parameter name	Value
Number of image blocks in training set N	10000
epochs	60
batch size	200
learning rate	1e-4
optimizer	RMSProp

The convergence of training process with *star-pattern* fabrics is shown in Figure 8. After 3000 iterations, the training loss value gradually decreases until convergence.

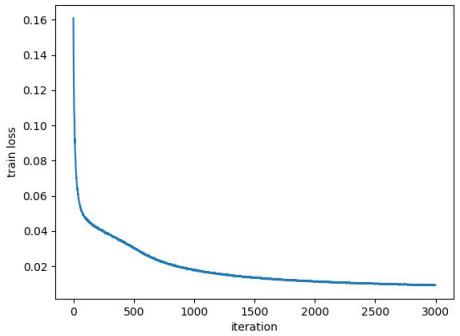

FIGURE 8. Convergence of training process.

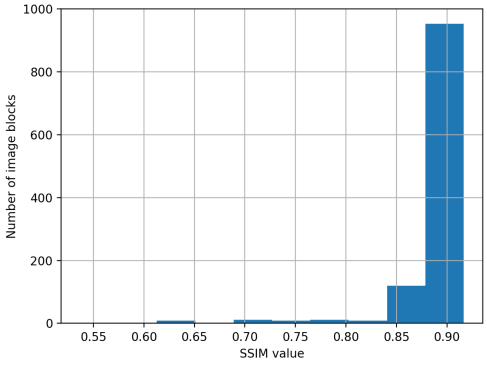

FIGURE 9. SSIM result histogram.

By constructing image pyramids, the features of image blocks can be more abundant. It makes the image

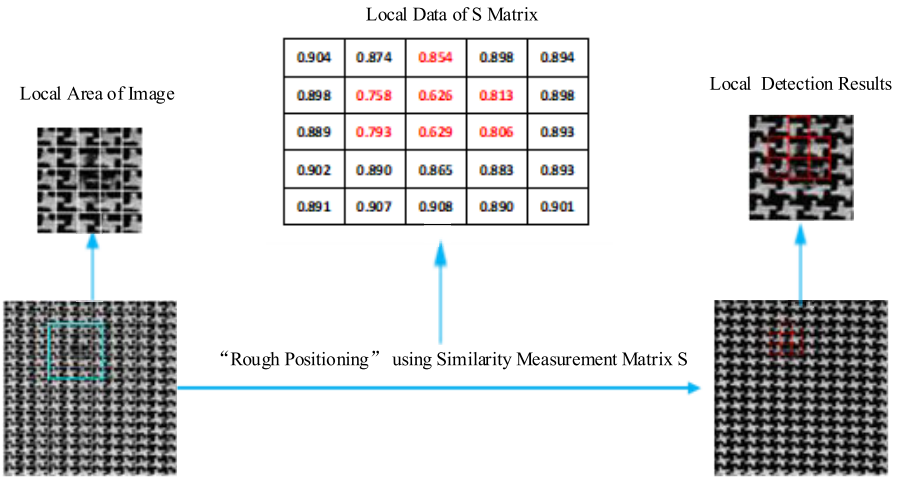

FIGURE 10. Schematic diagram of "rough-positioning."

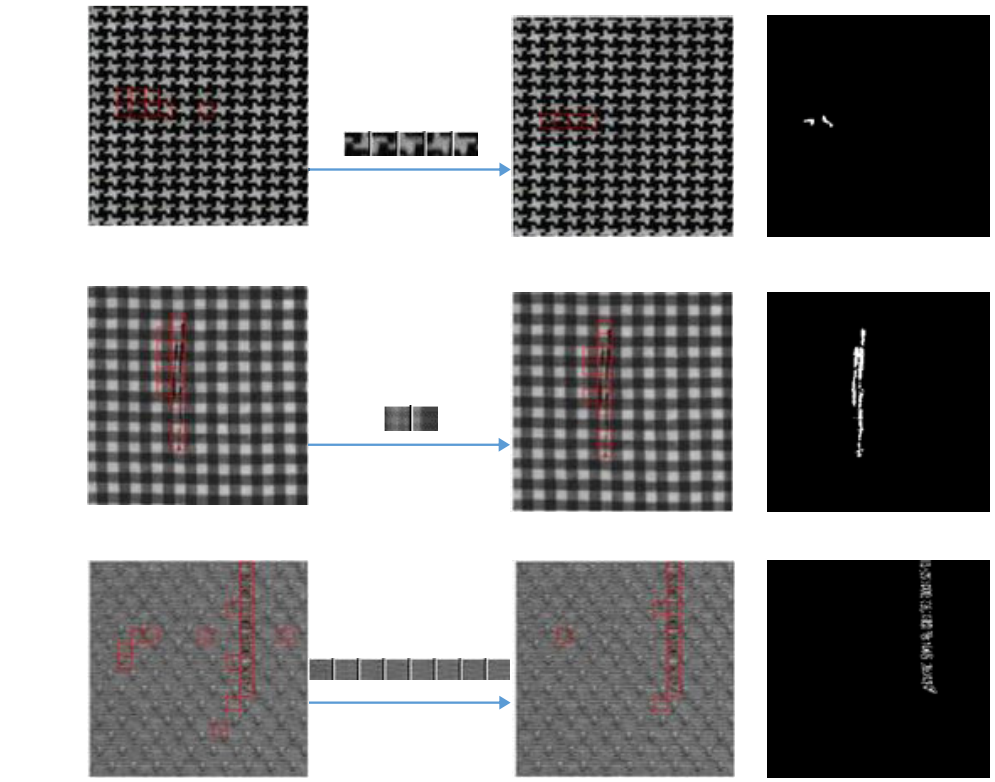

FIGURE 11. Results of "fine-positioning."

reconstruction ability of the improved model stronger, the defective blocks the similarity value between the defective blocks before and after reconstruction is smaller, and it is easier to judge whether they are defective blocks by similarity measurement.

C. DETERMINATION OF THE THRESHOLD

Threshold determination is directly related to the accuracy of detection. Threshold is determined from empirical studies.

We randomly extract 20% of each texture type images from the standard Periodic-pattern Fabric database to determine the threshold T_s and each image is divided into 256 image blocks. i.e. 1280 * image blocks of star type, 1280 * image blocks of box type and 1536 * image blocks of dot type are sampled respectively. Each image block corresponds to a structural similarity value. The structure similarity histogram of star texture type image blocks is shown in Figure 9.

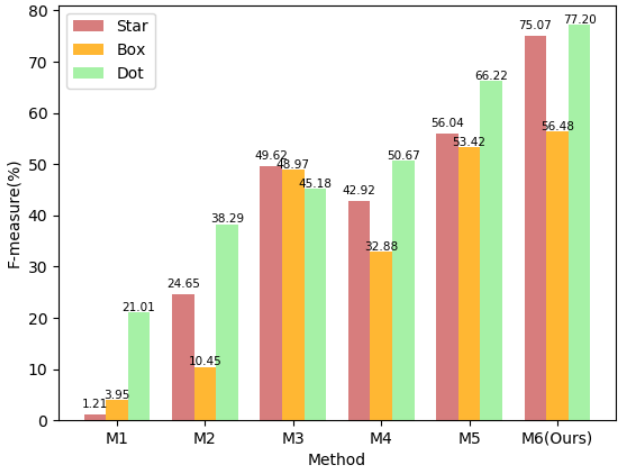

FIGURE 12. Detection results of six algorithms on periodic textured fabrics.

As it can be seen from Figure 9, the SSIM values of non defective image blocks are generally higher than those non-defective image blocks, most of which are above 0.80. In general, the threshold T_s, that is used to detect defective image blocks, is set to a number in the range of (0.80, 0.87). Because the threshold T_s is larger, more false detection blocks will be generated, at the same time, the missed detection rate can be effectively reduced. The threshold T_s is set 0.865. And the generated false detection blocks can be further filtered by the subsequent direction template matching process.

D. DEFECTS LOCALIZATION

The localization process for locating defective image blocks mainly consists of two steps: ''rough-positioning'' and ''fine- positioning.''

We use the self-similarity of image blocks to distinguish defective blocks from non-defective blocks for ''rough-positioning.'' The similarity measure matrix S of the image to be detected was calculated, and the threshold T_s was set to 0.865. Image blocks having self-similarity values less than T_s, are considered to be defective (as shown in Figure 10). After similarity measurement and ''rough-positioning'', defective blocks can be roughly located.

In the process of ''fine-positioning'', falsely detected image blocks from the ''rough-positioning'' process are further identified with respect to the local-similarity of the same column of image blocks. Thus, we select column template as reference template. Figure 11 (left) shows detection results obtained from the ''rough-positioning'' process (the red frame is the positioning block). Then, we calculate the direction template, match the image blocks of ''rough-positioning'' with the direction template in turn. We filter out these blocks with similarity values smaller than the threshold T_d, to obtain the result of the ''fine-positioning'' as shown in Figure 11 (middle). Finally, by comparing with the ground-truth in Figure 11 (right), the false detection rate of the ''fine-positioning'' results is lower than that of the ''rough-positioning'' results. The accuracy of the detection results is improved after using the template matching in column direction.

TABLE 2. Star fabric defect detection results (%).

Defect type	Method	TPR	FPR	PPV	NPV	F-measure
Broken end(5)	M1	0.26	3.56	0.09	99.24	0.13
	M2	8.79	1.16	7.17	99.27	7.89
	M3	70.86	**1.10**	26.09	99.70	38.14
	M4	87.22	2.39	21.51	99.90	34.51
	M5	**94.02**	2.14	20.99	**99.93**	34.31
	M6	89.90	3.09	**60.54**	99.58	**72.35**
Hole(5)	M1	0.34	3.66	0.05	99.45	0.09
	M2	24.47	1.23	11.68	99.54	15.81
	M3	59.27	**0.46**	41.82	99.79	49.22
	M4	90.86	1.59	23.98	99.95	37.95
	M5	**93.81**	1.08	31.91	**99.97**	47.62
	M6	84.33	2.06	**57.96**	99.59	**68.70**
Netting Multiple(5)	M1	1.03	3.61	0.88	98.25	0.95
	M2	16.42	0.82	12.61	98.54	14.26
	M3	59.80	**0.79**	55.03	99.43	57.32
	M4	**93.90**	2.68	38.44	**99.89**	54.55
	M5	86.80	1.14	53.24	99.70	65.99
	M6	79.11	1.39	**85.45**	98.94	**82.16**
Thick bar(5)	M1	4.37	3.44	5.09	96.63	4.70
	M2	69.52	1.67	54.52	98.81	61.11
	M3	53.58	0.61	54.75	98.07	54.16
	M4	53.51	2.28	45.91	98.31	49.42
	M5	**84.89**	**0.49**	**74.64**	**99.23**	**79.44**
	M6	74.75	1.91	73.65	98.26	74.19
Thin bar(5)	M1	0.00	3.65	0.00	99.00	None
	M2	45.47	2.83	12.50	99.45	19.61
	M3	65.52	**1.46**	29.56	99.77	40.74
	M4	**91.45**	4.04	18.22	**99.91**	30.39
	M5	86.00	3.39	23.57	99.94	36.99
	M6	69.93	1.86	**77.58**	98.05	**73.56**
Overall (25)	M1	1.20	3.58	1.22	98.51	1.21
	M2	32.93	1.54	19.70	99.12	24.65
	M3	61.81	**0.88**	41.45	99.35	49.62
	M4	73.93	2.59	30.24	99.59	42.92
	M5	**89.10**	1.65	40.87	**99.75**	56.04
	M6	79.60	2.06	**71.03**	98.88	**75.07**

E. DETECTION RESULTS AND COMPARISION

Ground-truth is divided into blocks. And 0 -1 operations are performed on the detected images, i.e., the detected defective

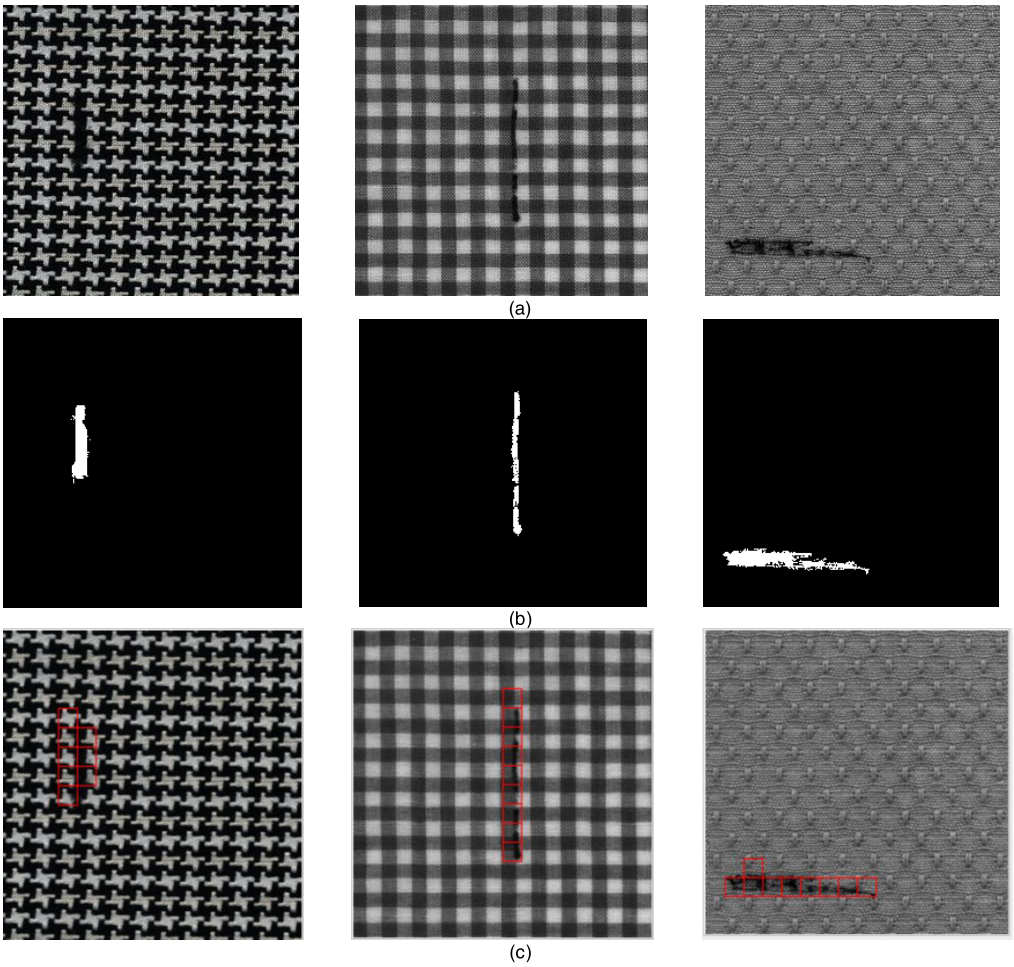

FIGURE 13. (a) Image to be detected. (b) Ground-truth. (c) Detection results of our method.

blocks are set to 1, and the rest is set to 0. The final detection results of our algorithm are compared with the corresponding ground-truth. True Positive (TP) is defined as both the detection results and the Ground-truth are 1. The parts marked with 0 in the detection results with their corresponding Ground-truth 0 are recorded as True Negative (TN). The parts marked with 1 in the detection results with their corresponding Ground-truth 0 are recorded as False Positive (FP). The parts marked with 0 in the detection results with their corresponding Ground-truth 1 are recorded as False Negative (FN). The four statistics above are used to calculate the following four evaluation indexes: True Positive Rate (TPR), False Positive Rate (FPR), Positive Predictive Value (PPV) and Negative Predictive Value (NPV).

$$TPR = TP/(TP + FN) \tag{2}$$

$$FPR = FP/(FP + TN) \tag{3}$$

$$PPV = TP/(TP + FP) \tag{4}$$

$$NPV = TN/(TN + FN) \tag{5}$$

A higher value of TPR, PPV & NPV or a lower value of FPR indicate better detection results.

Additionally, F-Measure index [33], [34] is used to evaluate the performance of the proposed methods. F-Measure is a comprehensive evaluation index used to measure the accuracy of two-category models in statistics. It also takes into account the accuracy of the classification model (also known as the precision of the PPV) and the recall rate (TPR). F-Measure can be seen as a weighted average of model accuracy and recall. It has a maximum value 1 and a minimum value 0. It is calculated as follows:

$$\mathrm{F-Measure} = \frac{2 \times PPV \times TPR}{PPV + TPR} = \frac{2 \times TP}{2 \times TP + FN + FP} \tag{6}$$

The performance of the proposed algorithm (labeled as M6) is compared with five well-known algorithms including WGIS, ER, [27], [28] and [29] (labeled as M1, M2, M3, M4, M5), with the respect to the five indicators mentioned above (TPR, FPR, PPV, NPV and F-Measure).

From the results shown in Table 2 to Table 4, it can be seen that the PPV of our method is 33.22% higher than other algorithms, on average (17.68% higher than M5 on average), which indicates that the defective block detection accuracy is

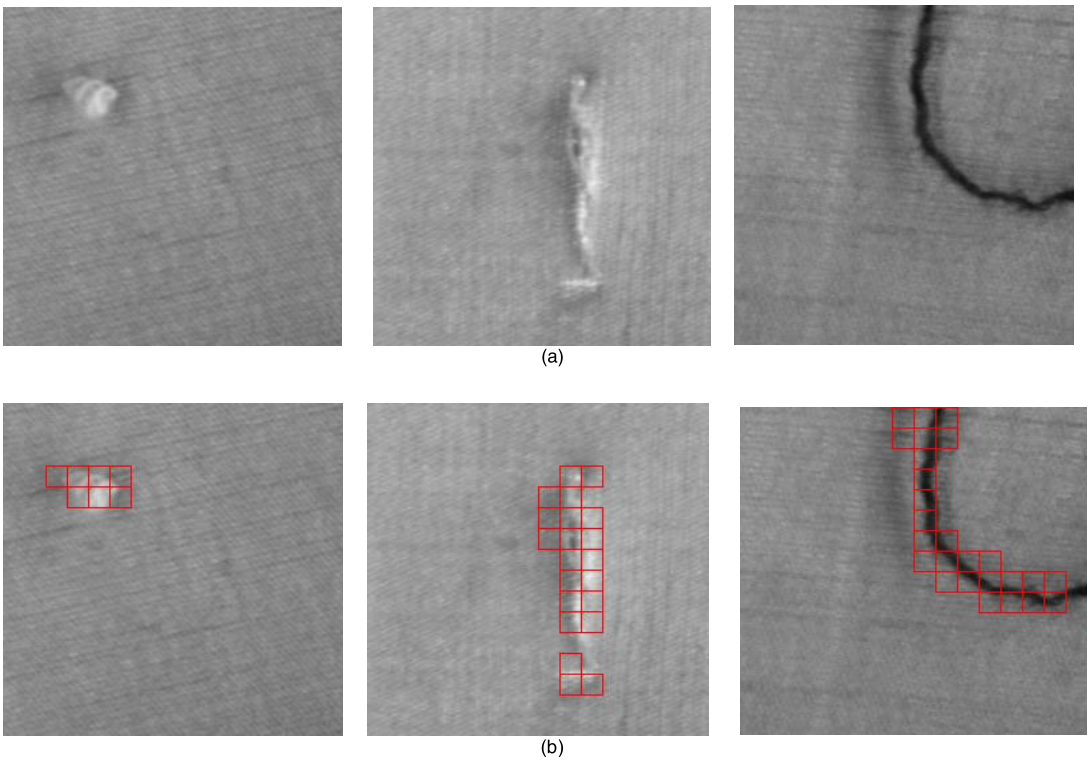

FIGURE 14. (a) Pure-color fabric images from TILDA dataset. (b)Defect detection results of (a).

higher than other methods. For the dot and star patterns, the average TPR and PPV values of the proposed algorithm are both above 70%. As shown in Figure 12, compared with the other five methods, the F-measure of the proposed algorithm is 26.28% higher than M1 – M4, on average (11.02% higher than M5 on average), which yields the best comprehensive performance. Compared with other methods, the precision (PPV) of the proposed method is significantly higher, but when detecting defects in star-pattern and box-pattern fabrics, the recall (TPR) is lower than the M5 method (down 3.81%) on average, FPR values are slightly less than the M5 method, which shows when the defect area is small, there are some errors in the detection result of our method. As it is shown in Table 3, the detection result of thick bar defect type in dot-pattern of our method is not as promising as others. The reason for this is to be investigated in the future work.

In addition, we also verified the effect of the chosen pyramid layers (4 layers in the experiments) and the image block size. As shown in Table 5 and Table 6, we can receive better results when the number of pyramid layers is set to 4 and the size of image block is set to 32*32.

Figure 13 shows the partial detection results of the proposed method from processing periodic-pattern fabric images. From Figure 13(b) and (c), it can be seen that the proposed method can accurately locate most of the defective blocks.

F. DETECTION RESULTS FOR PURE-COLOR FABRICS

As shown in Table 7, the proposed algorithm has been evaluated using the TILDA dataset, reaching 80.65% in F- Measure. The algorithm in this paper is not only effective for detecting defects in periodic-pattern fabrics, but it is also effective for detecting defects in pure-color fabrics without patterns. A part of the detection results is shown in Figure 14. Figure 14 (a) shows three pure-color fabrics with it is also effective for detecting defects in pure-color fabrics defects, while Figure 14 (b) shows the corresponding detection results. It can be seen that the proposed method can detect the location of the defective blocks more accurately.

G. ANALYSIS

When using the Periodic-pattern Fabric dataset, the proposed method can detect all 81 defects, in which 25 defects were detected from images containing star patterns, 26 detected from images containing box patterns and 30 detected from images containing dot patterns). Since the detection results of M3 and M4 methods contain more false positive image blocks (marked as non-defective and predicted as defective blocks), the final results of FPR and PPV are poor. Although the M5 method results in a better PPV and FPR due to the use of template correction and low rank decomposition methods, however, the M5 method is not suitable for fabrics with dot patterns, and its PPV index can be further improved. In this

TABLE 3. Box fabric defect detection results (%).

Defect type	Method	TPR	FPR	PPV	NPV	F-measure
Broken end(5)	M1	36.39	24.43	2.94	98.40	5.44
	M2	10.26	0.69	30.43	95.83	15.35
	M3	69.16	1.77	43.60	99.35	53.48
	M4	**81.79**	4.49	29.39	**99.57**	43.24
	M5	67.87	0.98	**56.58**	99.33	**61.71**
	M6	68.16	**0.42**	52.40	98.15	59.25
Hole (5)	M1	31.17	25.52	0.92	99.31	1.79
	M2	0.00	**0.03**	0.00	97.69	None
	M3	56.20	0.81	37.29	99.67	44.83
	M4	73.99	2.04	24.01	99.77	36.26
	M5	**79.57**	0.93	38.59	**99.83**	51.97
	M6	62.21	2.00	**58.92**	98.37	**60.52**
Netting Multiple(5)	M1	33.00	25.68	1.28	98.87	2.46
	M2	0.15	**0.04**	4.00	95.81	0.29
	M3	44.00	1.66	30.13	99.36	35.77
	M4	**61.82**	5.00	14.57	**99.45**	23.58
	M5	56.86	1.40	32.13	99.44	41.06
	M6	45.14	1.56	**50.80**	96.58	**47.80**
Thick bar(6)	M1	49.08	24.24	4.30	98.77	7.91
	M2	22.76	1.68	42.40	96.93	29.62
	M3	70.34	1.43	58.06	98.96	63.61
	M4	72.64	3.71	39.40	99.07	51.09
	M5	**79.17**	1.08	**62.59**	**99.75**	**69.91**
	M6	62.01	**0.93**	32.53	97.71	42.67
Thin bar (5)	M1	26.90	24.20	1.02	99.07	1.97
	M2	5.84	4.51	2.36	97.68	3.36
	M3	61.33	**1.90**	30.49	99.74	40.73
	M4	**95.30**	11.51	8.48	**99.94**	15.57
	M5	72.86	2.36	23.79	99.76	35.87
	M6	84.40	4.02	**56.88**	99.32	**67.96**
Overall (26)	M1	35.31	24.88	2.09	98.89	3.95
	M2	7.80	1.39	15.84	96.80	10.45
	M3	60.56	1.51	41.11	99.42	48.97
	M4	**76.34**	5.30	20.95	99.53	32.88
	M5	71.26	**1.35**	42.73	**99.60**	53.42
	M6	64.38	1.78	**50.30**	98.07	**56.48**

TABLE 4. Dot fabric defect detection results (%).

Defect type	Method	TPR	FPR	PPV	NPV	F-measure
Broken end(5)	M1	54.93	0.18	25.51	93.90	34.84
	M2	32.27	**0.01**	56.25	91.90	41.01
	M3	71.97	6.15	42.95	98.70	53.80
	M4	**94.27**	10.14	57.85	**99.07**	71.70
	M5	62.00	2.68	51.93	90.69	56.52
	M6	89.41	5.53	**71.11**	98.16	**79.22**
Hole(5)	M1	75.13	0.17	10.92	99.15	19.07
	M2	69.21	**0.05**	30.63	98.94	42.47
	M3	61.17	6.50	22.29	98.95	32.67
	M4	77.00	9.40	20.24	**99.22**	32.05
	M5	73.47	3.57	35.51	99.06	47.88
	M6	**81.03**	1.05	**94.21**	97.54	**87.12**
Netting Multiple(5)	M1	62.92	0.18	14.10	97.73	23.04
	M2	43.79	**0.01**	**80.95**	97.79	56.84
	M3	43.41	3.76	38.04	97.62	40.55
	M4	73.33	5.40	37.33	98.78	49.47
	M5	**82.29**	2.08	61.40	**99.18**	**70.33**
	M6	79.60	8.95	44.80	98.73	57.33
Knots (5)	M1	38.61	0.25	4.89	97.10	8.68
	M2	54.35	**0.01**	**66.88**	98.10	59.97
	M3	**77.72**	13.88	24.10	**99.02**	36.79
	M4	62.87	5.23	34.15	98.34	44.26
	M5	73.60	1.66	61.83	98.83	**67.20**
	M6	56.78	5.74	49.41	94.70	52.84
Thick bar(5)	M1	71.66	0.17	33.18	95.58	45.36
	M2	84.94	**0.15**	49.46	96.19	62.52
	M3	86.86	16.59	47.15	97.43	61.12
	M4	**97.86**	29.22	35.00	**99.52**	51.56
	M5	64.21	0.93	**90.14**	94.22	75.00
	M6	95.79	5.49	88.18	98.54	**91.83**
Thin bar(5)	M1	66.69	0.16	10.66	98.64	18.38
	M2	81.22	**0.07**	26.81	99.30	40.31
	M3	70.68	5.49	27.46	99.23	39.55
	M4	70.39	11.09	15.11	99.08	24.88
	M5	**94.26**	1.91	55.01	**99.80**	69.47
	M6	77.19	0.42	**100.00**	98.07	**87.13**
Overall (30)	M1	58.10	0.17	12.82	97.98	21.01
	M2	42.40	**0.04**	34.91	97.32	38.29
	M3	68.64	8.73	33.67	98.49	45.18
	M4	**87.28**	11.46	35.70	**98.96**	50.67
	M5	74.97	2.14	59.30	97.96	66.22
	M6	79.97	5.43	**74.61**	97.62	**77.20**

paper, the direction template matching method is used during the process of defect localization, which can effectively filter out some false positive image blocks, thus, improving PPV for all three kinds of fabrics.

Evaluations also consider recall rate, precision rate and F-Measure. When the recall rate is slightly reduced, the precision is significantly improved. The balanced index F-Measure of the proposed method is higher than all other methods involved in the evaluation.-The proposed method

TABLE 5. The detection results of our method with different pyramid layers (%).

Number of layers	TPR	FPR	PPV	NPV	F-measure
1	76.87	2.52	68.60	98.59	72.50
2	78.02	2.37	67.82	98.79	72.56
3	78.20	2.08	68.62	98.86	73.09
4(ours)	**79.60**	2.06	71.03	**98.88**	**75.07**
5	71.74	**1.92**	**71.47**	98.47	71.60
6	72.68	2.42	69.99	98.79	71.31

TABLE 6. The detection results of our method with different image block (%).

Size of image block	TPR	FPR	PPV	NPV	F-measure
16*16	73.46	3.15	65.64	98.22	69.33
24*24	62.38	3.35	58.53	98.29	60.39
32*32(ours)	79.60	2.06	71.03	98.88	75.07
40*40	44.78	4.50	65.53	94.43	53.20
48*48	40.78	4.52	63.54	94.84	49.67

TABLE 7. The detection results of our method on TILDA dataset (%).

TILDA	TPR	FPR	PPV	NPV	F-measure
Data1	86.68	3.79	85.26	98.65	85.96
Data2	85.70	3.37	73.56	99.21	79.17
Data3	79.89	1.05	73.63	95.92	76.63
Overall	84.09	2.74	77.48	97.93	80.65

has a strong potential to be applied to a wider range of applications.

V. CONCLUSION

A fabric defect detection method based on Image Pyramid and Direction Template is proposed in this paper. In the training stage, training sets are created by randomly extracting image blocks from non-defective images using image pyramids, which makes the feature information of the image block more abundant and the reconstruction effect of the model more remarkable. During the stage of image reconstruction and defect localization, the defective image blocks are roughly located by using the autocorrelation before and after reconstruction. The direction template is introduced to reduce the false detection rate of defective image blocks.

Experimental results show that the PPV index and the F-Measure index of the proposed method are much better than existing algorithms for periodic-fabric defect detection. The defect localization accuracy is better than other methods, achieved up to 69.58% on average for F-measure on Periodic-pattern Fabric database. And the algorithm can also be used for pure-color fabric defect detection, reaching 80.65% F-Measure for TILDA dataset. However, the proposed method achieves defect localization at block level. This can be further improved by detecting defects at pixel level.

ACKNOWLEDGMENT

The authors thank to the Industrial Automation Research Laboratory, Department of Electrical and Electronic Engineering, University of Hong Kong for providing the dataset and Nantong Yutong Textile Co., Ltd. for providing technical support. In addition, the authors thank to Dr. Dapeng Dong (Department of Computer Science, National University of Ireland, Maynooth) for improving the quality of this paper.

REFERENCES

[1] Y. L. Xi, Y. N. Zhang, and S. T. Ding, "Visual question answering model based on visual relationship detection," *Signal Process., Image Commun.*, vol. 80, pp. 115648-1–115648-14, Feb. 2020.
[2] K. Hanbay, M. F. Talu, and O. F. Ozguven, "Fabric defect detection systems and methods—A systematic literature review," *Optik*, vol. 127, no. 24, pp. 11960–11973, Dec. 2016.
[3] C. F. J. Kuo and H. M. Tu, "Gray relational analysis approach for the optimization of process setting in textile calendering," *Textile Res. J.*, vol. 79, no. 11, pp. 981–992, Jun. 2009.
[4] M. Kim, "Efficient histogram dictionary learning for text/image modeling and classification," *Data Mining Knowl. Discovery*, vol. 31, no. 1, pp. 203–232, Jan. 2017.
[5] D. Wang and H. Liu, "Edge detection of cord fabric defects image based on an improved morphological erosion detection methods," in *Proc. 6th Int. Conf. Natural Comput.*, Yantai, China, Aug. 2010, pp. 3943–3947.
[6] C.-H. Chan and G. K. H. Pang, "Fabric defect detection by Fourier analysis," *IEEE Trans. Ind. Appl.*, vol. 36, no. 5, pp. 1267–1276, Sep./Oct. 2000.
[7] Z. Kang, C. Yuan, and Q. Yang, "The fabric defect detection technology based on wavelet transform and neural network convergence," in *Proc. IEEE Int. Conf. Inf. Automat.*, Yinchuan, China, Aug. 2013, pp. 597–601.
[8] K. L. Mak and P. Peng, "An automated inspection system for textile fabrics based on Gabor filters," *Robot. Comput.-Integr. Manuf.*, vol. 24, no. 3, pp. 359–369, Jun. 2008.
[9] Y. Zhang, Z. Lu, and J. Li, "Fabric defect classification using radial basis function network," *Pattern Recognit. Lett.*, vol. 31, no. 13, pp. 2033–2042, Oct. 2010.
[10] D. Chetverikov, "Structural defects: General approach and application to textile inspection," in *Proc. Int. Conf. Pattern Recognit.*, Barcelona, Spain, Sep. 2000, pp. 521–524.
[11] J. Cao, J. Zhang, Z. Wen, N. Wang, and X. Liu, "Fabric defect inspection using prior knowledge guided least squares regression," *Multimedia Tools Appl.*, vol. 76, no. 3, pp. 4141–4157, Feb. 2017.
[12] H. Deng and D. A. Clausi, "Gaussian MRF rotation-invariant features for image classification," *IEEE Trans. Pattern Anal. Mach. Intell.*, vol. 26, no. 7, pp. 951–955, Jul. 2004.
[13] H. Y. T. Ngan, G. K. H. Pang, and N. H. C. Yung, "Ellipsoidal decision regions for motif-based patterned fabric defect detection," *Pattern Recognit.*, vol. 43, no. 6, pp. 2132–2144, Jun. 2010.
[14] W. B. Ouyang, B. G. Xu, and J. Hou, "Fabric defect detection using activation layer embedded convolutional neural network," *IEEE Access*, vol. 7, pp. 70130–70140, Jun. 2019.
[15] B. Wei, K. G. Hao, X. S. Tang, and L. H. Ren, "Fabric defect detection based on faster RCNN," in *Proc. Int. Conf. Artif. Intell. Textile Apparel*, HongKong, Jul. 2018, pp. 45–51.

[16] J. F. Jing, H. Ma, and H. H. Zhang, "Automatic fabric defect detection using a deep convolutional neural network," *Coloration Technol.*, vol. 135, no. 3, pp. 213–223, Mar. 2019.
[17] P. Napoletano, F. Piccoli, and R. Schettini, "Anomaly detection in nanofibrous materials by CNN-based self-similarity," *Sensors*, vol. 18, no. 1, pp. 209-1–209-15, 2018.
[18] B. Wei, K. G. Hao, and X. S. Tang, "A new method using the convolutional neural network with compressive sensing for fabric defect classification based on small sample sizes," *Textile Res. J.*, vol. 89, no. 17, pp. 3539–3555, Dec. 2018.
[19] S. Mei, H. Yang, and Z. Yin, "An unsupervised-learning-based approach for automated defect inspection on textured surfaces," *IEEE Trans. Instrum. Meas.*, vol. 67, no. 8, pp. 1266–1277, Jun. 2018.
[20] Y. Li, W. Zhao, and J. Pan, "Deformable patterned fabric defect detection with Fisher criterion-based deep learning," *IEEE Trans. Autom. Sci. Eng.*, vol. 14, no. 2, pp. 1256–1264, Apr. 2017.
[21] J. F. Jing, S. Chen, and P. F. Li, "Fabric defect detection based on golden image subtraction," *Coloration Technol.*, vol. 133, no. 1, pp. 26–39, Oct. 2016.
[22] H. Y. T. Ngan, G. K. H. Pang, S. P. Yung, and M. K. Ng, "Wavelet based methods on patterned fabric defect detection," *Pattern Recognit.*, vol. 38, no. 4, pp. 559–576, Apr. 2005.
[23] D.-M. Tsai, C.-P. Lin, and K.-T. Huang, "Defect detection in coloured texture surfaces using Gabor filters," *Imag. Sci. J.*, vol. 53, no. 1, pp. 27–37, Mar. 2005.
[24] M. K. Ng, H. Y. T. Ngan, X. Yuan, and W. Zhang, "Patterned fabric inspection and visualization by the method of image decomposition," *IEEE Trans. Autom. Sci. Eng.*, vol. 11, no. 3, pp. 943–947, Jul. 2014.
[25] M. Li, S. Wan, Z. Deng, and Y. Wang, "Fabric defect detection based on saliency histogram features," *Comput. Intell.*, vol. 35, pp. 517–534, Apr. 2019.
[26] C. S. C. Tsang, H. Y. T. Ngan, and G. K. H. Pang, "Fabric inspection based on the Elo rating method," *Pattern Recognit.*, vol. 51, pp. 378–394, Mar. 2016.
[27] J. Z. Liang, C. X. Gu, and X. Z. Chang, "Fabric defect detection based on similarity relation," *Pattern Recognit. Artif. Intell.*, vol. 30, no. 5, pp. 456–464, May 2017.
[28] W. Liu, X. Z. Chang, and J. Z. Liang, "Fabric defect detection based on local optimum analysis," *Pattern Recognit. Artif. Intell.*, vol. 31, no. 2, pp. 182–189, Feb. 2018.
[29] X. Ji, J. Z. Liang, and Z. J. Hou, "Fabric defect detection based on template correction and low-rank decomposition," *Pattern Recognit. Artif. Intell.*, vol. 32, no. 3, pp. 268–277, Mar. 2019.
[30] J. Yue, S. Mao, and M. Li, "A deep learning framework for hyperspectral image classification using spatial pyramid pooling," *Remote Sens. Lett.*, vol. 7, no. 9, pp. 875–884, Jun. 2016.
[31] B. Du, W. Xiong, J. Wu, L. Zhang, L. Zhang, and D. Tao, "Stacked convolutional denoising auto-encoders for feature representation," *IEEE Trans. Cybern.*, vol. 47, no. 4, pp. 1017–1027, Apr. 2017.
[32] Z. Wang, A. C. Bovik, H. R. Sheikh, and E. P. Simoncelli, "Image quality assessment: From error visibility to structural similarity," *IEEE Trans. Image Process.*, vol. 13, no. 4, pp. 600–612, Apr. 2004.
[33] N. Lazarevic-Mcmanus, J. Renno, and G. A. Jones, "Performance evaluation in visual surveillance using the F-measure," in *Proc. 4th ACM Int. Workshop Video Surveill. Sensor Netw.*, Santa Barbara, CA, USA, Oct. 2006, pp. 45–52.
[34] Y. J. Huang, R. Powers, and G. T. Montelione, "Protein NMR recall, precision, and F-measure scores (RPF scores): Structure quality assessment measures based on information retrieval statistics," *J. Amer. Chem. Soc.*, vol. 127, no. 6, pp. 1665–1674, Jan. 2005.

HUOSHENG XIE received the B.Sc. and M.Sc. degrees in computer science from Fuzhou University, China.

He is currently an Associate Professor with the School of Mathematics and Computer Science, Fuzhou University, China. He is also the Director of the Computer Experimental Teaching Center and a Senior Laboratory Engineer with the School of Mathematics and Computer Science, Fuzhou University. He has been a Principle Investigator of several Regional Natural Science Foundation projects, including the DNA-Protein Code Segmentation and Image Compression Algorithms. He is also an Associate Investigator of two National Science Foundation projects, conducting researches in the area of super-resolution blind image reconstruction, and 3-D cloud annotation. He is also a Principle Investigator of a joint project with textile industry, developing fabric defect detection algorithms. He is also collaborating with the Regional Weather Forecast Center conducting researches in AI-assisted weather forecast algorithms. His researches focus on computer vision, image processing, and virtual reality.

YAFENG ZHANG is currently pursuing the degree with the School of Mathematics and Computer Science, Fuzhou University. His research area is computer vision.

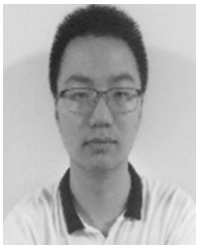

ZESEN WU is currently pursuing the degree with the School of Mathematics and Computer Science, Fuzhou University. His research area is computer vision.